Developmental Biology 448 (2019) 48–58

Contents lists available at ScienceDirect

Developmental Biology

journal homepage: www.elsevier.com/locate/developmentalbiology

Quantitative analysis reveals genotype- and domain- specific differences between mRNA and protein expression of segmentation genes in *Drosophila*

Svetlana Surkova[a,*], Alena Sokolkova[a], Konstantin Kozlov[a], Sergey V. Nuzhdin[a,b], Maria Samsonova[a,*]

[a] Peter the Great St. Petersburg Polytechnic University, Polytechnicheskaya, 29, St. Petersburg 195251, Russia
[b] Section of Molecular and Computational Biology, University of Southern California, Los Angeles 90089, CA, USA

ARTICLE INFO

Keywords:
Drosophila embryo
Segmentation genes
Gene expression
Confocal microscopy
mRNA and protein expression
Discrepancies between mRNA and protein levels
Pattern formation
Positional information

ABSTRACT

In many biological systems gene expression at mRNA and protein levels is not identical. Rigorous comparison of such differences on a spatio-temporal scale is still not feasible by high-throughput transcriptomic and proteomic analyses of early embryo development. Here, we characterize differences between mRNA and protein expression of *Drosophila* segmentation genes at the level of individual gene expression domains. We obtained quantitative imaging data on expression of gap genes *gt* and *hb* and pair-rule gene *eve* for *Drosophila* wild type embryos, *Kr* null mutants and *Kr+/Kr-* heterozygotes. To compare mRNA and protein expression we use several criteria including difference in amplitude and positions of expression domains, pattern shape and positional variability. For a number of gene expression domains we show examples where protein expression does not repeat mRNA expression even after a temporal delay. We calculated time delays between *eve* pattern formation at the level of mRNA and protein for wild type embryos, *Kr* mutants and *Kr+/Kr-* heterozygotes. We detect that in wild type embryos, the amplitudes of *eve* stripes 3 and 7 do not differ significantly at the level of mRNA, however, stripe 3 is higher than stripe 7 at the protein level. We further show that *hb* mRNA and protein expression in both anterior and posterior domains significantly differs at specific time points. The formation of *hb* PS4 stripe at the mRNA level proceeds five times faster than at the level of protein. With regard to spatial expression, we show that the offset between posterior *gt* mRNA and protein domains is much larger in *Kr* mutants than in wild type embryos and heterozygotes. Finally, we analyze differences in positional variability of *eve* stripe 7 expression in *Kr* mutants and *Kr+/Kr-* heterozygotes at the level of mRNA and protein. These results enable further perspectives to uncover mechanisms underlying discrepancies between mRNA and protein expression in early embryo.

1. Introduction

Until recently, it has been common practice to consider gene expression at the level of mRNA as a main determinant of protein abundance. However, genome-wide analysis revealed that in a wide range of organisms correlation between mRNA and protein levels is not strong. Results often show correlation coefficients around 0.40, which implies that only 40% of the variation in protein concentration can be explained by knowing mRNA abundances (Maier et al., 2009; de Sousa Abreu et al., 2009; Vogel and Marcotte, 2012). Along with transcriptional regulation, there are many other levels of gene expression control, including mRNA processing, translational regulation, regulation of protein stability and degradation. Exact contributions of regulation at the RNA level versus regulation at the protein level are subject to ongoing debate (Schwanhäusser et al., 2011; Li et al., 2014; Koussounadis et al., 2015; Cheng et al., 2016; Liu et al., 2016). Rigorous comparison of differences between mRNA and protein expression on a spatio-temporal scale is still not feasible by high-throughput transcriptomic and proteomic analyses and consequently requires acquisition of quantitative data in situ.

Traditionally, segmentation process in fruit fly *Drosophila* is regarded as one of the primary model systems to study regulatory interactions underlying pattern formation. Before maternal-to-zygotic transition (MZT), maternally deposited transcripts and proteins are regulated post-transcriptionally. Mechanisms of position-dependent translational regulation of maternally expressed mRNAs, leading to

* Corresponding authors.
E-mail addresses: surkova_syu@spbstu.ru (S. Surkova), m.samsonova@spbstu.ru (M. Samsonova).

https://doi.org/10.1016/j.ydbio.2019.01.006
Received 18 February 2018; Received in revised form 12 December 2018; Accepted 4 January 2019
Available online 07 January 2019
0012-1606/ © 2019 Elsevier Inc. All rights reserved.

establishment of molecular gradients underlying embryonic pattern in early *Drosophila* embryo, were intensively studied during last two decades (Lasko, 2011). Bicoid (Bcd) protein gradient represses translation of evenly distributed *caudal (cad)* mRNA in the anterior region of *Drosophila* embryo and forms the posterior Cad gradient. Later in development, Cad gradient serves as a main activator of posterior zygotic gene expression. Similarly, Nanos (Nos) protein prevents maternal *hunchback (hb)* translation in the posterior. This forms Hb anterior gradient which is necessary for the correct establishment of gap gene domain borders (Dubnau and Struhl, 1996; Rivera-Pomar et al., 1996; Sonoda and Wharton, 1999; Chagnovich and Lehmann, 2001; Niessing et al., 2002; Cho et al., 2006; Lasko, 2011).

Following the onset of zygotic transcription during MZT, transcriptional networks control a progressive refinement of gap and pair-rule gene expression domains. This finally leads to the precise determination of parasegmental borders. *Drosophila* segmentation gene network is well studied and currently serves as a good model for understanding molecular mechanisms of eukaryotic transcription (Jaeger and Manu, 2012; Jaeger, 2011; Bothma et al., 2014; Fukaya et al., 2016).

Despite large amount of studies on translational and transcriptional regulation in *Drosophila* early embryo, existing publications mostly lack a comprehensive comparison of mRNA and protein spatial patterns after the onset of zygotic transcription. We found the following evidence for the domain-specific differences between mRNA and protein expression in this system.

Earlier studies showed that the borders of gap gene *Kruppel (Kr)* expression domain were less sharp at protein level compared to the mRNA level (Gaul et al., 1987). Later on, asymmetric distribution of mRNA relative to protein in posterior gap domains was explained by mutual transcriptional repression of gap genes (Jaeger et al., 2004, see below). Further evidence was that *hunchback (hb)* gene expression in PS4 stripe, responsible for formation of *Drosophila* mesothoracic (T2) segment, was better pronounced at the mRNA level (Wu et al., 2001).

A recent quantitative study revealed similar tendencies in dependency between mRNA and protein expression levels for the posterior domains of gap genes *Kr*, *knirps (kni)* and *giant (gt)* (Becker et al., 2013). In these domains, mRNA and protein expression patterns are remarkably similar in shape. However, the authors detect significant differences between mRNA and protein concentrations. mRNA expression reaches maximum in mid-cycle 14A and then sharply decreases. Protein expression reaches its maximum 15–20 min later than mRNA and retains high levels until the end of cleavage cycle 14A (onset of gastrulation). Delay between mRNA and protein expression in general comprises mRNA processing, export from the nucleus and translation into protein. Using mathematical modeling approach, the authors test whether post-transcriptional regulation is required for correct expression of gap protein domains. The results suggested that post-transcriptional regulation is not required for patterning in this system, however, it is necessary for proper control of protein concentrations (Becker et al., 2013).

Differences in spatial positions of posterior gap domains between mRNA and protein were also reported (Jaeger et al., 2004; Becker et al., 2013). They manifest in asymmetric expression of mRNA with respect to protein which leads to significant differences in positions of posterior domain borders in wild type embryos. This asymmetry is caused by the transcriptional repression directed from neighboring gap domains located more posteriorly and drives spatial shifts of posterior domains in the anterior direction (Jaeger et al., 2004; Jaeger, 2011).

Combination of spatial shifts of *even skipped (eve)* stripes with time delays for protein synthesis also leads to more anterior mRNA distribution with respect to protein domains in wild type embryos from mid-late cycle 14A (Clark, 2017).

In this paper, we quantitatively characterize differences between mRNA and protein expression of three segmentation genes in *Drosophila* early embryo by comparing amplitude, shape, positional shifts and variability of gene expression domains at the level of mRNA and protein. Recent studies reveal differential changes in mRNA and protein expression in response to experimental perturbations (Maier et al., 2011; Jovanovic et al., 2015; Cheng et al., 2016). We use null mutation in *Kr* gene as a perturbing factor and analyze mRNA and protein expression in wild type embryos and mutants. We obtained data on expression of gap genes *gt* and *hb* and the pair-rule gene *even skipped (eve)* for wild type embryos, *Kr* null mutants and *Kr+/Kr-* heterozygotes, including double staining of embryos for mRNA and protein.

Several questions remain unanswered. First, does the shape of protein patterns always reproduce the shape of mRNA patterns even after a temporal delay? Second, is it reliable to predict protein concentration within gene expression domain from its mRNA concentration? In silico studies often use a transcript pattern as a proxy for the protein pattern and vise versa. We highlight cases where using transcript patterns would yield unambiguously wrong protein patterns at specific time points.

Our paper presents the detailed quantitative comparison of the domain-specific mRNA and protein expression of three *Drosophila* segmentation genes. For several domains these quantities are measured simultaneously. Some recent publications provide evidence that protein expression could be explained as a function of mRNA expression despite poor correlation between mRNA and protein abundances (e.g. Peshkin et al., 2015), while the other studies suggest requirement of post-transcriptional regulation in *Drosophila* embryogenesis (Becker et al., 2018). Given this ambiguity, our results can provide interesting perspectives to uncover mechanisms underlying differences between mRNA and protein spatial expression in early embryos.

2. Materials and methods

2.1. Collecting and staining of embryos

Drosophila melanogaster wild type (Oregon R), *Kr-* (Kr^1 amorphic allele (Wieschaus et al., 1984)) and *Kr+/Kr-* embryos were collected and fixed as described elsewhere (Surkova et al., 2008a, 2013). Embryos were stained for *hb*, *gt* and *eve* mRNA expression using the two-stage HCR method, which includes hybridization and amplification (modified from Choi et al., 2014, see Supplementary protocol). Probes were designed by Molecular Instruments (http://www.molecularinstruments.org/) to target all transcripts of examined segmentation genes at cellular blastoderm stage. After HCR, most of embryos were stained with antibodies against protein products of *gt* and *hb*, which were gifts of John Reinitz and Mark Biggin (Surkova et al., 2008a, 2013). In this case ProteinaseK treatment at the hybridization step was replaced by incubation with 80% acetone for 10 min at −20 °C (Nagaso et al., 2001). This method was effective and kept good quality of mRNA staining. Finally, embryos were stained with Hoechst 34580 DNA dye (ThermoFisher) for 8–10 min to mark the nuclei, and then mounted in the Prolong gold antifade mountant (ThermoFisher).

2.2. Confocal microscopy and image segmentation

Laterally oriented embryos from cleavage cycle 14A were imaged using confocal microscope Zeiss 700 (Translational Imaging Center, USC) with the 20X objective. Two-six optical sections were scanned through the surface nuclei with the distance of 1 μm. Each section was averaged 8 times.

Parameters of confocal microscope (gain and offset) for *hb* mRNA and protein were calibrated as described earlier (Surkova et al., 2008a). Consequently, for *hb* we consider raw intensity extracted from confocal images. For mRNA expression of *eve* and *gt* "gain" parameter of the microscope was adjusted during scanning to avoid pixel saturation. In order to bring expression levels to the universal scale, we normalized quantitative data using the intensity of *eve* stripe 1 and *gt* second

anterior domain respectively. This method of normalization is reliable, because it completely reproduces previously published dynamics of Gt posterior domain amplitude both in wild type and *Kr* mutant embryos (Surkova et al., 2008a, 2013), as well as the dependency between *gt* mRNA and protein concentrations in wild type (Becker et al., 2013).

After fluorescent imaging, we scanned sagittal sections in transmitted light to check the degree of cell membrane invagination for further precise detection of developmental age of the embryos (Surkova et al., 2013).

Image stacks were segmented in ProStack software (https://sourceforge.net/projects/prostack/) (Kozlov, 2008) using several pipelines, which sequentially apply different image processing tools and finally create binary masks of the whole embryo and embryonic nuclei (Surkova et al., 2008b). Whole embryo mask was used to put embryo into correct orientation and to crop image according to the embryo dimensions. Nuclear masks provided information on spatial positions of centroids and average fluorescence intensity within each nucleus, finally formatted as Excel tables.

2.3. Processing of quantitative data

Removal of nonspecific background signal, extraction of characteristic features of expression patterns, spatial registration and data integration were performed in the BREReA software (https://sourceforge.net/projects/brerea/). We used the anterior-posterior (A–P) positions of expression maxima as well as points where expression is 50% of maximum ("domain borders") as characteristic quantitative features. We analyzed gene expression profiles from the central 10% dorsoventral (D-V) stripe extracted along the A-P axis (Surkova et al., 2008a, 2013).

We classified the quantitative data on gene expression into 8 time classes approximately 6.5 min each according to the degree of cell membrane invagination and dynamic changes in gene expression (Surkova et al., 2008a, 2013). These data were used for the construction of integrated (averaged) patterns to capture overall dynamics of gene expression.

To estimate statistical significance of spatial shifts and variability we used more generalized classification and merged each of two neighboring temporal classes into four time groups ((1–2), (3–4), (5–6) and (7–8)) with a time resolution of about 13 min each.

To compare distances between gene expression domain borders at the level of mRNA and protein we performed the unpaired *t*-test at a confidence level of $P = 0.05$. Pearson correlation coefficients were calculated to test the similarity of *eve* mRNA and protein expression patterns in different time classes. Normality of distributions was checked using Lilliefors and Shapiro-Wilk tests.

2.4. The dataset

2.4.1. Our new dataset includes 139 Drosophila embryos

Below is the distribution of embryos according to genotype and stained gene product: (a) wild type (wt) embryos: *eve* mRNA (N = 45); *gt* mRNA (N = 54); *hb* mRNA (N = 36); Hb protein (N = 20); Gt protein (N = 13). (b) *Kr* null mutants: *eve* mRNA (N = 37); *gt* mRNA (N = 31); Hb protein (N = 13), Gt protein (N = 12). (c) *Kr*+/*Kr*- heterozygotes: *eve* mRNA (N = 41); *gt* mRNA (N = 37); Hb protein (N = 17), Gt protein (N = 19).

35 embryos were stained for the expression of *gt, hb* and *eve* at the level of mRNA in the following combinations: *gt* mRNA, *hb* mRNA and *eve* mRNA (22 wt embryos) and *gt* mRNA and *eve* mRNA (13 embryos: 7 *Kr*-, 3 *Kr*+/*Kr*- and 3 wt). 104 embryos were stained simultaneously for mRNA and protein products of the following genes: *gt* mRNA, Hb protein and *eve* mRNA (36 embryos: 13 *Kr*-, 17 *Kr*+/*Kr*- and 6 wt); *gt* mRNA, Gt protein and *eve* mRNA (44 embryos: 12 *Kr*-, 19 *Kr*+/*Kr*- and 13 wt); *gt* mRNA, *hb* mRNA, Hb protein and *eve* mRNA (12 embryos: 5 *Kr*-, 4 *Kr*+/*Kr*- and 3 wt) and Hb protein and *hb* mRNA (12wt embryos).

Quantitative and integrated data can be uploaded from https://doi.org/10.5281/zenodo.2228371. All other data types are available from authors.

We combined these new data with the earlier obtained data on protein expression (Surkova et al., 2008a, 2013). Supplementary Table S5 shows the number of embryos used for the construction of data plots.

3. Results

3.1. Stripe-specific differences between eve mRNA and protein expression

3.1.1. Correlation between eve expression patterns at the level of mRNA and protein

We obtained the quantitative dataset on *eve* mRNA expression for wild type embryos, *Kr* null mutants and *Kr*+/*Kr*- heterozygotes and compared it with protein expression (Supplementary Figs. S1–S3). During cleavage cycle 14A *eve* expression is highly dynamic and patterns change their shape very quickly. While in gap domains mRNA and protein patterns differ mostly by the level of expression (Becker et al., 2013), in *eve* such differences can be judged from the pattern shape which includes the intensity of stripes, time, sequence and type of formation (Surkova et al., 2008a). This criterion is nearly independent from experimental error, i.e. background staining, variation in concentration of antibodies/probes or settings of the confocal microscope.

We sought to understand, whether the shape of *eve* protein patterns repeats the shape of the corresponding mRNA patterns, and if so, what is the temporal delay between pattern formation at the level of mRNA and protein. A visual inspection of integrated data on *eve* expression reveals that in wild type embryos from early cycle 14A, protein patterns nearly reproduce mRNA patterns with a delay of one time class, or about 6.5 min of development (Fig. 1A-F, Fig. 1H,I and Supplementary Fig. S1). Indeed, *eve* mRNA patterns from time classes 1 and 2 have maximum values of correlation with the protein patterns from time classes 2 and 3 respectively (Fig. 1G and Table 1). For time classes 3–5 the delay increases to two time classes or approximately 13 min (Supplementary Fig. S1 and Table 1). In *Kr*+/*Kr*- heterozygotes from time classes 3–5, and in *Kr*- embryos from time classes 2–3, protein patterns also form with a delay of ~13 min (Supplementary Tables S1 and S2). In *Kr*- embryos from mid-cycle 14A, all mRNA patterns show the best correlation with protein patterns from time class 5 (Supplementary Table S2). Presumably, this is due to the complicated shape of *eve* patterns in mutants (Supplementary Fig. S2). However, by the end of cycle 14A, *eve* patterns at the level of mRNA and protein attain nearly similar shapes and this is observed in all genotypes (Supplementary Figs. S1–S3).

3.1.2. eve stripe 7 expression is increased at the level of mRNA in early-mid cycle 14A

Detailed comparison of individual *eve* stripes (Supplementary Figs. S1–S3) revealed that *eve* stripe 7 is increased at the level of mRNA compared to that of protein in early-mid cycle 14A (Fig. 1L-N). This increase is especially pronounced in *Kr* null mutants and *Kr*+/*Kr*- heterozygotes and is evident both for averaged patterns (Fig. 1M,N and Supplementary Figs. S1–S3) and for *eve* profiles in individual embryos (Fig. 1O-P).

We plotted mRNA and protein maximum concentrations of *eve* stripe 7 for the time groups (1–2) – (7–8) (Fig. 1Q-S). Note, that the spatial positions of *eve* stripe 7 maximum differ between mRNA and protein levels as stripe 7 shifts significantly over time and this movement is not identical for the mRNA and protein patterns (see Fig. 4C,D and Supplementary Figs. S1–S3).

In wild type embryos and *Kr* mutants from time group (1–2), mRNA expression in *eve* stripe 7 is significantly increased compared to protein expression (Fig. 1Q,S). This difference is maximized in time group (3–4). While stripe 7 maximum expression at the level of mRNA

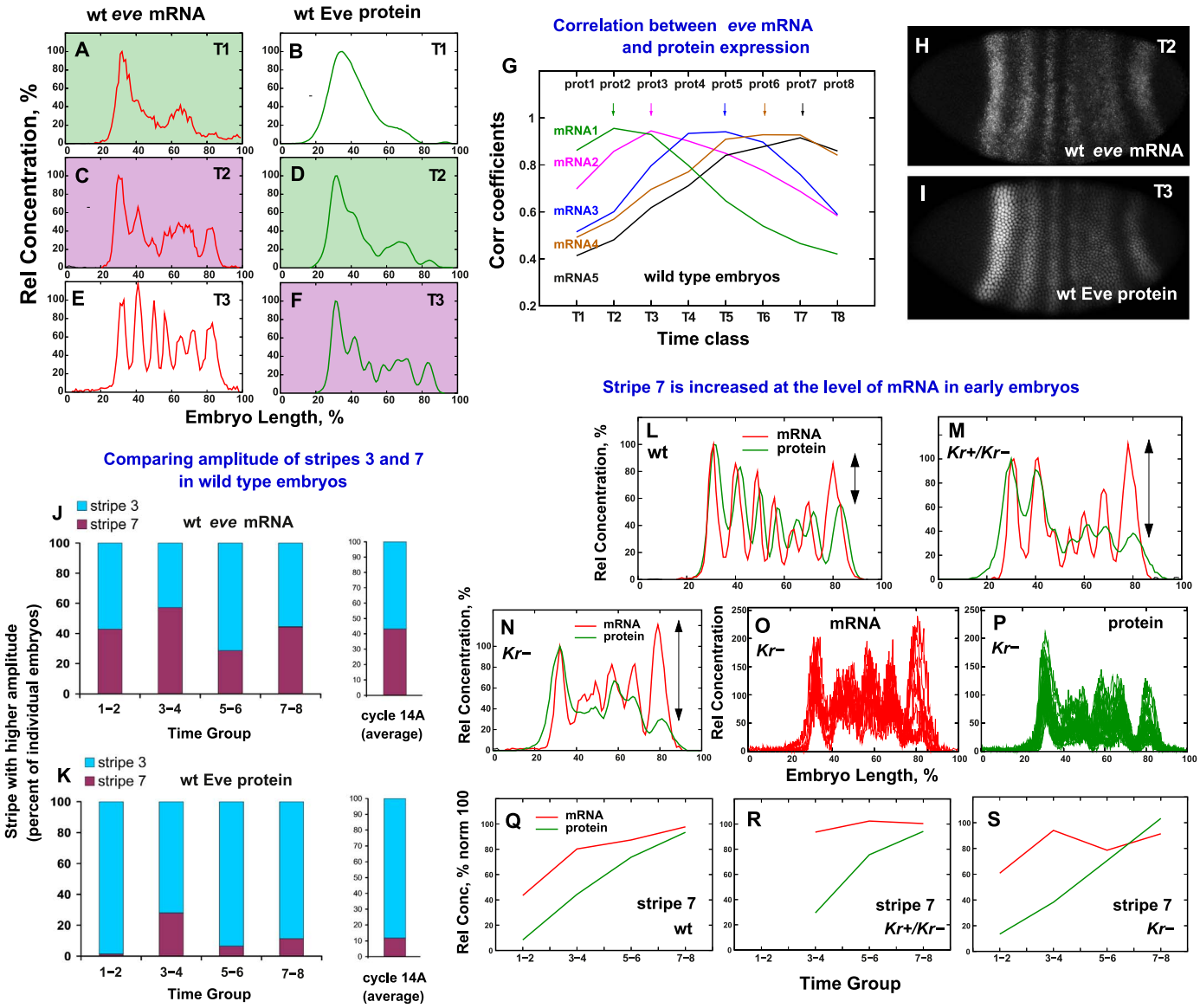

Fig. 1. Stripe-specific differences in the levels of *eve* mRNA and protein expression. (A-F) Averaged patterns of *eve* expression in wild type embryos from time classes 1–3. mRNA and protein patterns with similar shape are marked by the same colors. (G) Correlation coefficients for *eve* mRNA patterns from time classes 1–5 (colored curves) and Eve protein patterns from time classes 1–8. Protein patterns show maximum correlation with mRNA patterns in time classes marked by arrows. (H, I) Confocal images of *eve* expression in wild type embryos from time classes 2 and 3 stained for mRNA (H) and protein (I) respectively. Images show very similar expression patterns. (J, K) Amplitudes of *eve* stripes 3 and 7 are compared for each individual wild type embryo at the level of mRNA (J) and protein (K). Bar graphs show percent of embryos with higher stripe 3 (light bars) or 7 (dark bars) in each time group (left-hand graphs) and averaged data for cycle 14A (right-hand graphs). (L, M) Averaged patterns show increased *eve* mRNA expression in stripe 7 in wild type embryos (L), *Kr+/Kr-* heterozygotes (M) and *Kr* null mutants (N) from time group (3–4). Arrows show difference in amplitude of stripe 7 between protein and mRNA patterns. (O, P) Examples of *eve* expression profiles before normalization in 8 individual *Kr* mutant embryos from time group (3–4) at the level of mRNA and in 27 randomly chosen *Kr* mutant embryos at the level of protein. (Q-S). Dynamics of *eve* mRNA and protein concentrations in stripe 7 during cycle 14A in wild type embryos (Q), *Kr+/Kr-* heterozygotes (R) and *Kr* null mutants (S).

increases sharply in early times, its protein expression rises gradually until gastrulation. By the end of cycle 14A, mRNA and protein amplitudes become more similar (Fig. 1Q,S). For *Kr+/Kr-* heterozygotes, *eve* mRNA and protein maximum concentrations show the same tendency, although the data is only available starting from time group (3–4) (Fig. 1R).

3.1.3. Difference between amplitudes of eve stripes 3 and 7 is more pronounced at the level of protein

We decided to compare the amplitudes of *eve* stripe 7 and stripe 3 in individual wild type embryos at the level of mRNA and protein. Expression of both stripes is driven by *eve*3+7 enhancer (Small et al., 1996; Clyde et al., 2003; Struffi et al., 2011) and stripe 7 is additionally regulated by an *eve*2+7 regulatory sequence (Janssens et al., 2006; Staller et al., 2015).

Although stripes 3 and 7 have different spatial dynamics within *eve* pattern, namely, stripe 7 significantly shifts in the anterior direction over time (Fig. 4C,D, Surkova et al., 2008a), we used maximum amplitude of these stripes as a criteria to compare mRNA and protein levels. For each time group, we estimated percent of individual embryos where stripe 3 is higher than stripe 7 (light bars), or conversely, where stripe 7 is higher than stripe 3 (dark bars) (Fig. 1J,K). At mRNA level (Fig. 1J), the proportion of embryos with elevated stripe 3 or elevated stripe 7 varies from about 71% and 29% to 57% and 43% respectively depending on the time group. For all cycle 14A, this proportion is 57% and 43% (right-hand graph) on average, demonstrating almost equal balance between stripe 3 and 7 amplitudes.

However, at the protein level, the proportion of embryos with elevated stripes 3 or 7 varies from 99% and 1% to 72% and 28% (about 88% and 12% on average) (Fig. 1K).

Table 1
Temporal correlation between *eve* mRNA and protein expression patterns in wild type embryos. Table shows Pearson correlation coefficients for averaged *eve* mRNA patterns from time classes 1–8 and corresponding protein patterns. Shaded cells show maximum values of correlations. All coefficients are statistically significant ($P < 0.05$). Normality of distributions was checked using Lilliefors and Shapiro-Wilk tests.

eve	PROT T1	PROT T2	PROT T3	PROT T4	PROT T5	PROT T6	PROT T7	PROT T8
mRNA T1	0.8619	0.9557	0.9297	0.7975	0.6472	0.54	0.4651	0.4205
mRNA T2	0.6976	0.8576	0.9447	0.9015	0.8489	0.7764	0.6871	0.5828
mRNA T3	0.5149	0.6007	0.7961	0.934	0.9411	0.8967	0.7592	0.5886
mRNA T4	0.4915	0.5691	0.6962	0.7704	0.9092	0.9285	0.9273	0.8412
mRNA T5	0.4136	0.4809	0.6178	0.7114	0.8404	0.877	0.9151	0.8593
mRNA T6	0.3202	0.4006	0.5506	0.6696	0.8545	0.9204	0.9491	0.8304
mRNA T7	0.2291	0.2929	0.3475	0.3279	0.346	0.3758	0.4992	0.7041
mRNA T8	0.3265	0.3595	0.3932	0.3782	0.3868	0.3871	0.4456	0.6173

We can conclude that the difference in maximum amplitudes between stripes 3 and 7 is pronounced at the protein level, where stripe 3 is higher than stripe 7 in the majority of embryos, but not at the level of mRNA.

3.1.4. Discrepancies between mRNA and protein expression in hb anterior and posterior domains

Zygotic *hb* expression is complex. In early times zygotic *hb* is expressed in a broad anterior domain which is under the control of the Bcd morphogen gradient (Driever and Nusslein-Volhard, 1989). Later in development, two new domains arise: the posterior domain and the PS4 stripe, which is responsible for the formation of the T2 segment (Fig. 2A-E, Wu et al., 2001).

Since PS4 stripe forms in cleavage cycle 14A, we were able to compare the rate of its formation in individual wild type embryos at the level of mRNA and protein (Fig. 2F). At the mRNA level, formation of this stripe proceeds very quickly. It starts in time class 2 and is finished by time class 3. Formation of the PS4 stripe at the protein level starts in time class 4 (~13 min later) and proceeds during time classes 4–8 (Fig. 2F). This comprises about 33 min of development, which is five times longer than at the level of mRNA. Thus, there is a significant delay between PS4 stripe formation at mRNA and protein levels.

In order to understand whether *hb* mRNA pattern can be used as a proxy for Hb protein pattern, we analyzed *hb* mRNA and protein expression in the anterior and posterior domains. Dynamics of mRNA and protein concentrations in the *hb* anterior domain in general resemble the previously described dynamics of *Kr, gt* and *kni* posterior domains (Becker et al., 2013), although *hb* anterior mRNA declines at the earlier times and more sharply. Hb anterior protein expression, on the contrary, remains high until gastrulation (Fig. 2G, Supplementary Fig. S4).

Unlike anterior expression, the maximum amplitude of posterior *hb* mRNA domain sharply increases until time group (3–4) and then slightly declines, while protein expression increases gradually until the end of cycle 14A (Fig. 2G).

hb posterior domain has the similar shape at mRNA and protein levels and the only difference between mRNA and protein expression is the sharp increase in the mRNA amplitude in early time groups (Fig. 2D,E,G). On the contrary, Hb anterior protein expression does not repeat the shape or amplitude of its mRNA expression even after a temporal delay (Fig. 2D-G).

3.2. Genotype-specific differences of posterior gt expression at the level of mRNA and protein

3.2.1. gt posterior mRNA domain in Kr mutants is displaced with respect to protein domain

As previously shown, the expression domains of zygotic genes dynamically change their spatial positions after their initial setting by the threshold concentrations of maternal gradients (Jaeger et al., 2004; Surkova et al., 2008a; El-Sherif and Levine, 2016). In the posterior domains of gap genes, these shifts are driven by asymmetric repression between neighboring domains, which is directed from the more posteriorly located domain. For posterior *Kr, kni* and *gt* domains in wild type embryos, this leads to the asymmetric spatial distribution of mRNA in relation to protein (Jaeger et al., 2004; Becker et al., 2013).

Posterior *gt* domain provides interesting clues for understanding the dynamic interpretation of positional information in early embryo (Jaeger et al., 2004). During cleavage cycle 14A this domain shifts in the anterior direction on more than 8% of embryo length (EL) in wild type embryos and on more than 13% EL in *Kr* null mutants (Surkova et al., 2013). These values are equal to 8 and 13 embryonic nuclei along the A-P axis respectively.

In accordance with previous studies (Jaeger et al., 2004; Becker et al., 2013), we detect that in wild type embryos, *gt* mRNA is distributed asymmetrically with respect to its protein product. The posterior border of *gt* mRNA domain ("post") is located anteriorly in relation to its protein border (white bar on Fig. 3A and black arrows on Fig. 3C). *Kr+/Kr-* heterozygotes also show this asymmetry (black arrows on Fig. 3D).

Surprisingly, in *Kr* mutants, both anterior ("ant") and posterior ("post") borders of *gt* mRNA domain are shifted with respect to protein domain borders (black arrows on Fig. 3E). Mismatch in the anterior border positions is evident in individual *Kr* mutant embryos double stained for *gt* mRNA and protein (white "ant" bar on Fig. 3B). Interestingly, prior to gastrulation, positions of *gt* mRNA and protein borders in *Kr* mutants converge, unlike those in wild type embryos (Fig. 3E).

The statistical significance of these observations was estimated by co-staining 43 individual embryos from cycle 14A for *gt* mRNA and protein (Tables 2A and B). As expected, in wild type and heterozygous embryos, we detect asymmetry of *gt* mRNA distribution with respect to protein (Table 2A), which is statistically significant ($p < 0.05$, Table 2B (a and b)).

In *Kr* mutants, the *gt* mRNA domain is shifted in relation to the protein domain on about 4.8 nuclei at the anterior border and on about 4.4 nuclei at posterior border (Table 2A). These distances do not significantly differ from each other (Table 2B (c)), however, they significantly differ from distances between corresponding borders in wild type embryos and heterozygotes (Table 2B (e,f and h,i)). Thus, in *Kr* mutants mRNA distribution with respect to protein distribution is less asymmetric than in wild type embryos and heterozygotes. Detailed comparisons are provided in the legend of Table 2B.

To conclude, the anterior displacement of *gt* posterior mRNA expression relative to protein expression in *Kr* mutants is much larger than in wild type embryos and heterozygotes. It constitutes about one-third of *gt* domain width and is mostly pronounced in early time classes (Fig. 3B,E, Supplementary Fig. S6).

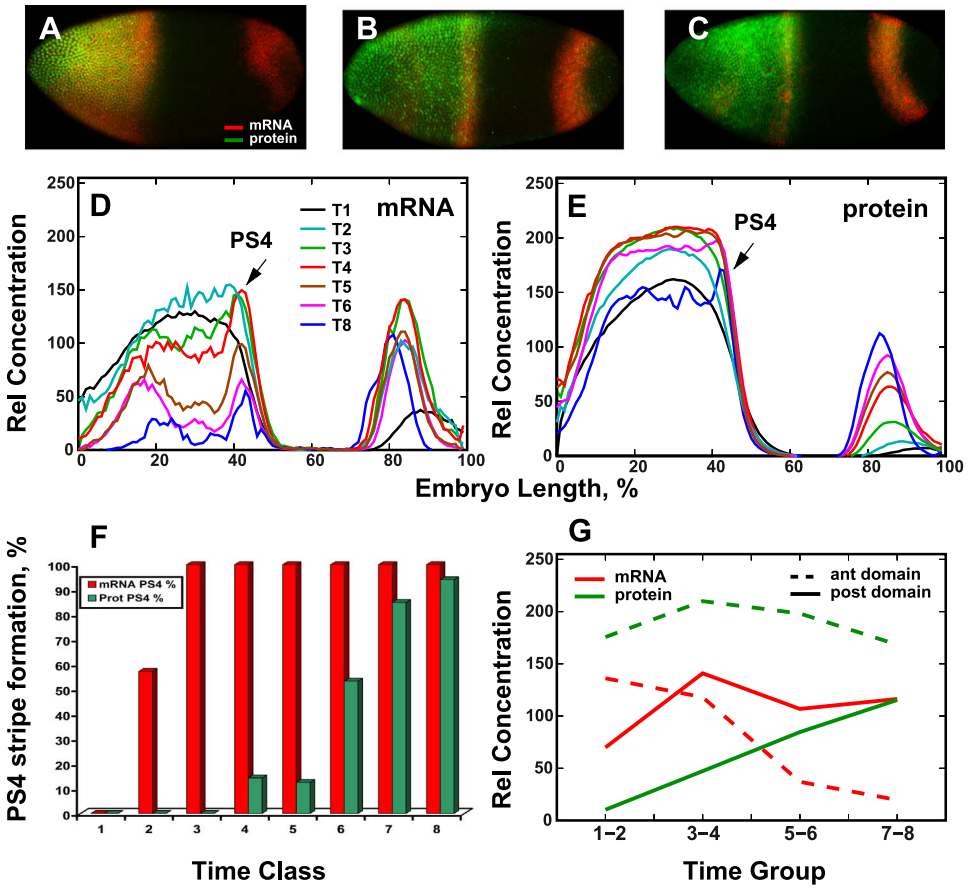

Fig. 2. Domain-specific differences between *hb* mRNA and protein expression. (A-C) Individual wild type embryos from time classes 1, 5 and 8, double stained for *hb* mRNA and Hb protein. (D, E) Integrated patterns of *hb* mRNA (D) and protein (E) expression in wild type embryos. Arrow shows PS4 stripe. (F) Rate of PS4 stripe formation in individual embryos at the level of mRNA and protein. For each time class, bar graph shows percent of embryos where PS4 stripe has already formed. (G) Temporal dynamics of *hb* intensity for the anterior domain (at its midpoint) and for posterior domain maximum.

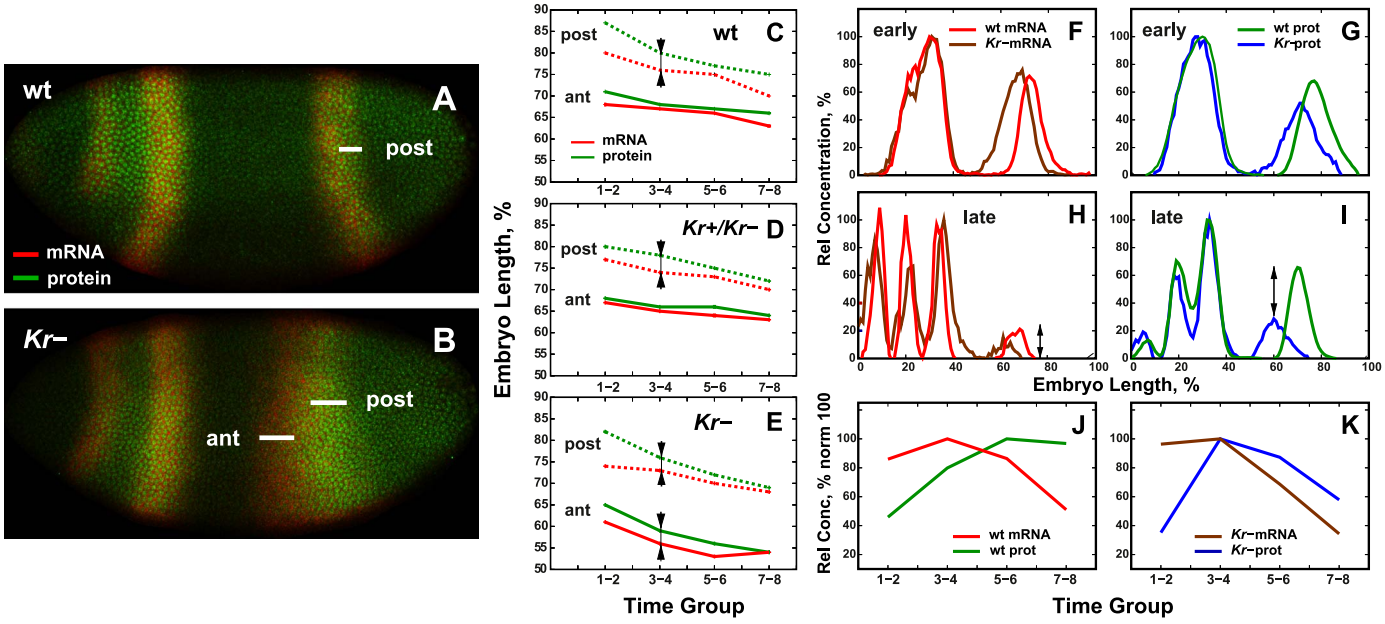

Fig. 3. Differences between *gt* mRNA and protein expression in wild type embryos and *Kr* mutants. (A-B) A mismatch between the posterior (post) and anterior (ant) border positions of *gt* posterior domain at mRNA and protein levels (white bars). Individual wild type (A) and *Kr* mutant (B) embryos were double stained for *gt* mRNA and protein. (C-E) Dynamics of averaged positions of *gt* posterior domain borders at the level of mRNA and protein for wild type (C), *Kr*+/*Kr*- (D) and *Kr*- embryos (E). Black arrows show difference between mRNA and protein positions for anterior and posterior borders respectively (see also Tables 2A and B). (F-I) Integrated patterns of *gt* expression at the level of mRNA (F, H) and protein (G, I) in wild type and *Kr*- embryos from time classes 2 and 8. Arrow on panel H shows that by the end of cycle 14A *gt* posterior mRNA expression declines both in wild type and *Kr*- embryos. On the contrary, Gt posterior protein expression declines only *Kr* mutants (arrow on I).(J, K) Temporal dynamics of posterior *gt* mRNA and protein concentrations (shown as percent maximum) in wild type embryos (J) and *Kr* mutants (K).

3.2.2. Wild type embryos and Kr mutants show similar mRNA levels but different protein levels within the gt posterior domain in late cycle 14A

According to previously published results, in wild type embryos, the posterior *gt* mRNA expression reaches its maximum in early cycle 14A and then sharply declines, while protein expression retains high levels until gastrulation (Becker et al., 2013; Surkova et al., 2013) (Fig. 3J). Our data confirm this observation (Fig. 3F-I, J). Interestingly, in *Kr* mutants, both mRNA and protein maximum concentrations within *gt* posterior domain decline in the second half of cleavage cycle 14A (Fig. 3F-I, K). Thus, in late cycle 14A we observe low mRNA concentrations both in wild type embryos and *Kr* mutants, however, low protein concentration are detected only in mutants (Fig. 3H,I). We can assume that the fast spatial displacement of *gt* mRNA domain (Fig. 3B) may account for the decrease in Gt protein amplitude in mutant embryos.

Table 2A
Distances between *gt* protein and mRNA domain borders in individual embryos. Distances between the A-P positions of *gt* posterior domain borders at the level of protein and mRNA are shown in percent embryo length (EL). Values of distances were calculated for 43 individual embryos double stained for *gt* mRNA and protein, and then averaged for wild type embryos (WT), *Kr+/Kr-* heterozygotes (HET) and *Kr* null mutants (MUT). "A border" and "P border" are anterior and posterior borders respectively.

***gt* genotype**	**A** border	**P** border
	Distances between border positions at the level of mRNA and protein (in % EL)	
WT (N = 12)	0.09	2.05
HET (N = 19)	0.81	1.97
MUT (N = 12)	**4.79**	**4.39**

3.3. Spatial dynamics and positional variability of mRNA and protein expression in Kr+/Kr- heterozygotes

As we have previously shown, the shape and A-P width of the early Eve protein patterns in *Kr+/Kr-* heterozygotes resemble those in *Kr* null mutants, but by the end of cycle 14A, Eve expression becomes very similar to wild type, thus dynamically correcting the mutant phenotype (Surkova et al., 2013).

Here, we analyzed the positional dynamics of posterior *gt* domain and *eve* stripe 7 in *Kr+/Kr-* heterozygotes at the level of mRNA and protein. We detect that by the end of cycle 14A positions of expression domains at the level of mRNA in heterozygotes nearly coincide with those in wild type embryos (Fig. 4A,C). At the level of protein, the correction of domain positions in *Kr+/Kr-* embryos is not fully manifested, although the tendency of dynamic shifts toward wild type positions is clearly evident (Fig. 4B,D).

We have previously reported that the variability in positions of the Gt posterior protein domain decreases during cleavage cycle 14A both in wild type embryos and *Kr* mutants, providing the precise patterning by gastrulation (Surkova et al., 2013). In *Kr+/Kr-* heterozygotes, *gt* positional variability follows the same tendency both at the level of mRNA and protein (Supplementary Table S4).

On the contrary, the positional variability of Eve stripe 7 at the protein level was low in wild type embryos but remained high in *Kr* mutants throughout all cleavage cycle 14A (Surkova et al., 2013). Here we detect that in early cycle 14A, *Kr+/Kr-* heterozygotes also show high variability in Eve stripe 7 positions at the protein level. Unlike *Kr* mutants, this variability decreases over time, however, by the end of cleavage cycle 14A it remains essentially higher than in wild type embryos (Fig. 4E, Supplementary Table S3).

Interestingly, at the level of mRNA, *eve* stripe 7 is also very variable both in *Kr+/Kr-* heterozygotes and *Kr* null mutants in the early cycle

Table 2B
Statistical comparison of distances between *gt* posterior domain borders at the level of mRNA and protein from Table 2A. Distances for anterior (A) and posterior (P) borders reflect the degree of asymmetry of mRNA distribution relative to protein distribution. Distances in each row are compared using unpaired *t*-test, statistically significant comparisons are shaded in gray ($P < 0.05$). (1) Within-genotype comparison. For wild type embryos (WT) and *Kr+/Kr-* heterozygotes (HET) difference between indicated distances is statistically significant (1a,b). In *Kr* null mutants (MUT) distances do not differ significantly (1c) and this means that in mutants Gt protein domain is shifted less asymmetrically with respect to *gt* mRNA domain. (2,3) Between-genotype comparison. Distances for anterior (2) or posterior (3) borders of *gt* posterior domain do not differ significantly between wild type embryos and *Kr+/Kr-* heterozygotes. However, both A and P distances in *Kr* mutants differ significantly form those in wild type embryos and heterozygotes.

		Pair-wise comparison of distances between border positions of *gt* posterior domain at the level of mRNA and protein (from Table 2A)		**Statistical significance**
1	a	**A** border **WT**	**P** border **WT**	0.0080
	b	**A** border **HET**	**P** border **HET**	0.0332
	c	**A** border **MUT**	**P** border **MUT**	0.5992
2	d	**A** border **WT**	**A** border **HET**	0.2303
	e	**A** border **MUT**	**A** border **WT**	<0.0001
	f	**A** border **MUT**	**A** border **HET**	<0.0001
3	g	**P** border **WT**	**P** border **HET**	0.8969
	h	**P** border **MUT**	**P** border **WT**	0.0043
	i	**P** border **MUT**	**P** border **HET**	0.0018

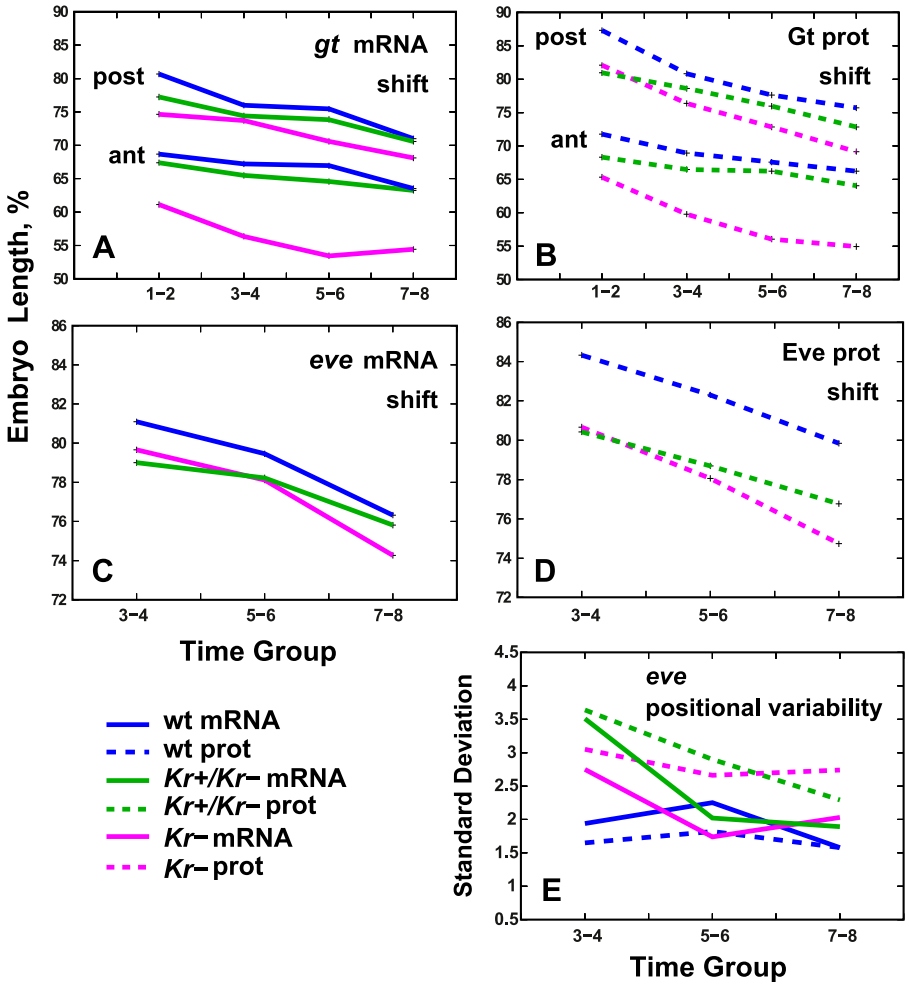

Fig. 4. Dynamic correction of spatial positions of expression domains in *Kr+/Kr-* heterozygotes is better pronounced at the level of mRNA. Dynamic shifts in positions of anterior (ant) and posterior (post) borders of *gt* posterior domain (A,B) and *eve* stripe 7 maximum (C,D) are shown at the level of mRNA and protein. (E) Standard deviations in positions of *eve* stripe 7 maximum.

14A. However, over the course of development, this variability sharply declines and attains nearly the same level as in wild type embryos (Fig. 4E).

Taken together, these results show that the correction of mutant phenotype is better pronounced at the level of mRNA than at the protein level.

4. Discussion

In this paper, we quantitatively compared mRNA and protein expression of three segmentation genes in *Drosophila* early embryo. Protein expression is closer to phenotype than mRNA expression, thus the discrepancies between mRNA and protein expression in early embryos can potentially have patterning implications. Some recent studies provide evidence that protein expression could be explained as a function of mRNA expression (Peshkin et al., 2015; Becker et al., 2013), while the other publications demonstrate the requirement of post-transcriptional regulation in *Drosophila* embryogenesis (Becker et al., 2018).

Here, we show the specific examples where protein expression of *Drosophila* segmentation genes does not recapitulate mRNA expression even after the temporal delay. We analyze a number of spatio-temporal discrepancies between mRNA and protein expression, including differences in shape, amplitude and positional variability of gene expression domains. In silico studies often use protein expression as a proxy for mRNA expression and vise versa. We highlight cases where such approach can lead to unambiguously wrong predictions. For the specific gene expression domains, the correct results may be obtained only when both mRNA and protein concentrations are measured directly.

Mechanisms underlying the observed discrepancies between transcript and protein expression in the *Drosophila* blastoderm should be further investigated.

4.1. Domain- and genotype- specific differences between mRNA and protein temporal and spatial expression

A quantitative study by Becker et al. reported similar dynamics in expression levels for posterior domains of gap genes *Kr, kni* and *gt*. Concentration of mRNA reached maximum in early cycle 14A and then significantly declined, while protein levels peaked with the delay of 15–20 min and remained high until gastrulation (Becker et al., 2013). Our analysis of maximum mRNA and protein amplitudes within *Kr, kni* and *gt* domains supports this observation. This is schematically shown in Fig. 5A. The similarity in both in mRNA and protein expression dynamics of posterior *Kr, kni* and *gt* is predictable because all these domains appear nearly simultaneously at cleavage cycles 11–12 and have equal shapes. The question is: what is the time delay between mRNA and protein expression during formation of more complex patterns (e.g. in pair-rule genes) and how is it affected by mutations?

We examined the dynamically forming early *eve* patterns and detected that, in general, protein patterns reach the shape of mRNA

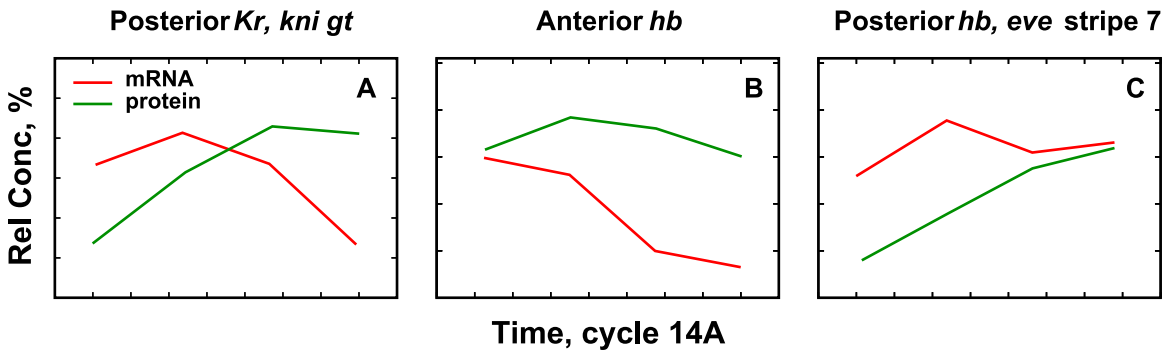

Fig. 5. Domain-specific temporal changes in mRNA and protein maximum expression levels. (A) mRNA expression in posterior *Kr, kni* and *gt* domains reaches maximum in early cycle 14A and declines thereafter. Protein reaches maximum with a delay of 2–3 time classes (~13–20 min) (Becker et al., 2013 and this paper). (B) mRNA concentration in the anterior *hb* domain sharply declines in early cycle 14A, however, protein retains high levels until gastrulation. (C) Posterior *hb* domain and *eve* stripe 7 show sharp increase of mRNA in early cycle 14A, while protein expression increases gradually until gastrulation.

patterns with the delay of one-two time classes (~6.5–13 min). Surprisingly, in early cycle 14A, amplitude of *eve* stripe 7 at the mRNA level is significantly increased compared to the protein amplitude. This increase is evident in wild type embryos (Fig. 1L,Q) but is most pronounced in *Kr* null mutants and *Kr+/Kr-* heterozygotes (Fig. 1M-P, R,S).

Moreover, comparison of stripe 7 intensity with that of stripe 3 in individual wild type embryos revealed that stripe 3 is higher than stripe 7 in the majority of embryos at the protein level (Fig. 1K). However, at the level of mRNA, the amplitudes of these stripes do not differ significantly (Fig. 1J). Transcription in these stripes is only partially regulated by a common *eve*3+7 enhancer, as stripe 7 is under the additional control of the *eve*2+7 regulatory sequence (Clyde et al., 2003; Struffi et al., 2011; Janssens et al., 2006; Staller et al., 2015). Thus, we could expect larger difference between mRNA expression of stripes 3 and 7, however we observe difference only in their protein levels. One possible explanation comes from the observation that stripe 7 is more dynamic than stripe 3, as it shifts significantly over time in the anterior direction (Fig. 4C,D). Therefore, the high levels of transcription in *eve* stripe 7 may be more transient in each nucleus and as a consequence lead to low levels of protein expression in this stripe.

With respect to the early increase of mRNA expression of eve stripe 7 compared to its protein expression (Fig. 1Q-S), our results show that such elevation is also inherent to *hb* posterior domain (Fig. 2G, Fig. 5C). In both cases, mRNA expression sharply increases in early cycle 14A, but does not significantly decline thereafter and retains the same level as the protein. Remarkably, in the related species *D. pseudoobscura* and *D. yakuba*, increased mRNA intensity in the posterior domains of *hb* and *eve* is much more pronounced than in *D. melanogaster* (Fowlkes et al., 2011 (Fig. 2), Tautz and Nigro, 1998 (Fig. 4)).

As this mode is inherent to stripes located near the posterior pole of the embryo, we can assume its functional role. In *Drosophila,* the posterior pair-rule stripes are often formed later than the anterior ones. Consequently, in order to reach appropriate amplitude by the time of segment determination, they require increased levels of mRNA to provide active protein synthesis. Delayed pattern formation of posterior stripes in *Drosophila* presumably has evolved from the short germband insects, where segments are not formed simultaneously, but are added sequentially at the posterior growth zone (Damen, 2007). Molecular mechanisms underlying regulatory connections between posterior patterning during long and short (intermediate) germ-band segmentation are actively studied (Clark, 2017).

The anterior domain of *hb* shows fundamentally different dynamics than the posterior domain. In this case, mRNA expression dynamically decreases to very low levels, but protein is retained at high concentrations (Figs. 2A-E, G and 5B). Both mRNA and protein dynamics somehow resemble those of the posterior *Kr*, *kni* and *gt* domains in the second half of cycle 14A (Fig. 5A). From a functional point of view, maintenance of high protein concentration within the anterior Hb protein is quite important as this domain plays a fundamental role in segment determination by activating *eve* stripe 2 and setting borders both of gap domains and *eve* stripe 3. At the same time, high levels of Hb protein may contribute to the sharp decline of anterior *hb* mRNA (Fig. 2D,E) due to self-repression reported in some studies (Xu et al., 2015).

4.2. Shape of expression patterns at the level of mRNA and protein

In wild type embryos and *Kr+/Kr-* heterozygotes in early-mid cycle 14A, Eve protein stripes reproduce the pattern of *eve* mRNA stripes after a delay (Fig. 1A-F, G and Supplementary Figs. S1 and S3). Although we find some inconsistencies in correlations between *eve* mRNA and protein expression in *Kr* mutants from mid-cycle 14A (Supplementary Table S2), in late cycle 14A *eve* protein and mRNA patterns reach almost similar shapes in all genotypes (Supplementary Figs. S1–S3, Table 1, Supplementary Tables 1 and 2). By this time, *eve* turns from stripe-specific regulation by gap genes to the refinement of whole patterns directed by the late element (Goto et al., 1989; Harding et al., 1989). The refined *eve* stripes are required to ensure the stability of the future parasegment boundaries (Fujioka et al., 2002).

Protein expression in the posterior *gt* and *hb* domains also becomes very similar in shape to the corresponding mRNA expression after temporal delays, which are domain-specific (Fig. 5A,C). Thus, mRNA and protein expression of posterior gap domains differs only by intensity levels in the particular time class. This is in agreement with the earlier published results (Becker et al., 2013).

On the contrary, anterior *hb* and *gt* protein expression does not attain the shape of mRNA expression even prior to gastrulation (Fig. 2A-E, Supplementary Figs. S4, S5 and S6). Moreover, we found that formation of the *hb* PS4 stripe at the level of mRNA proceeds five times faster than at the level of protein (Fig. 2F).

Thus, in contrast to posterior gap domains, the anterior domains show significant discrepancy in a shape between mRNA and protein expression. This phenomenon deserves further investigation.

4.3. Spatial displacement of mRNA expression in relation to protein expression

For *Drosophila* embryos, we compared spatial positions of the *gt* posterior domain at the level of mRNA and protein in wild type embryos, *Kr+/Kr-* heterozygotes and *Kr* null mutants.

In wild type embryos and heterozygotes, posterior *gt* mRNA expression is distributed asymmetrically in relation to protein distribution, leading to the difference in positions of posterior borders (Fig. 3C,D, Tables 2A and B).

Remarkably, in *Kr* mutants, *gt* mRNA is displaced anteriorly with

respect to Gt protein domain on more than 4 nuclei that constitutes about one third of its width (Fig. 3B,E, Tables 2A and B). This displacement is caused by the fast movement of the *gt* mRNA expression domain in the anterior direction, driven by Hb repression from the posterior, absence of Kr domain in the anterior and very low concentration of Knirps (Kni) (Kozlov et al., 2012). Gt protein expression in *Kr* mutants finally attains the same positions as mRNA, but with a delay, which is presumably required for protein accumulation (Fig. 3E).

Interestingly, during cleavage cycle 14A, *gt* mRNA concentration in the posterior domain declines abruptly both in wild type embryos and *Kr* mutants (Fig. 3H). However, Gt protein decreases significantly only in mutants (Fig. 3I). Although the transcriptional regulatory mechanisms of *gt* domain decrease in *Kr* mutants have been revealed by the earlier *in silico* study (Kozlov et al., 2012), we can hypothesize that the discrepancy in positions between posterior *gt* mRNA and protein expression in mutants (Fig. 3B,E) may additionally account for the decrease of Gt protein concentration.

4.4. Dynamic correction of spatial domain positions in Kr+/Kr- heterozygotes is better pronounced at the level of mRNA

A recent study suggests a crucial role for the domain shifts in correct segment determination in insects (Clark, 2017). In our dataset, we were able to compare the spatial dynamics of gene expression in wild type embryos, *Kr+/Kr-* heterozygotes and *Kr* null mutants at the level of mRNA and protein. We analyzed *gt* and *eve* posterior domains which shift significantly over time.

In our previous work, we detected that the shape and width of *eve* expression patterns in *Kr+/Kr-* heterozygotes in early cycle 14A resemble those in *Kr* null mutants. However, later on, these traits tend to become similar to those in wild type (Surkova et al., 2013).

Analysis of dynamic shifts in both the posterior *gt* domain and *eve* stripe 7 in *Kr+/Kr-* heterozygotes shows the same tendency. In heterozygous embryos from early cycle 14A, *gt* and *eve* domains are positioned more anteriorly, like in null mutants. However, as development proceeds, these domains move toward wild type positions (Fig. 4A-D). In general, this effect can be explained by the dynamic increase of low Kr concentrations to the half-normal levels, sufficient to correct the mutant phenotype.

Interestingly, in *Kr+/Kr-* heterozygotes at the end of cycle 14A, the domain positions at the mRNA level are closer to their wild type positions than the positions of these domains at the level of protein (Fig. 4A-D). Moreover, the analysis of positional variability of *eve* stripe 7 in heterozygotes and *Kr* null mutants revealed that it decreases over time at the mRNA level (Fig. 4E). However, at the protein level, the variability decreases to a lesser extent in heterozygotes (Fig. 4E) and remains high in *Kr* mutants (Surkova et al., 2013). Thus, in *Kr+/Kr-* heterozygotes, the spatial positions of expression domains at the protein level are not fully corrected by the time of segment determination, and although heterozygotes are viable, this can result in segmentation defects observed later in development (Bullock et al., 2004).

Acknowledgements

This work was supported by Russian Foundation for Basic Research (RFBR) Grant 17-04-01665-a and National Institutes of Health Grant U01GM103804. We would like to thank Sammi Ali for help with improving the manuscript and Srna Vlaho for the assistance with maintenance of fly stocks.

Appendix A. Supporting information

Supplementary data associated with this article can be found in the online version at doi:10.1016/j.ydbio.2019.01.006.

References

Becker, K., Balsa-Canto, E., Cicin-Sain, D., Hoermann, A., Janssens, H., Banga, J.R., Jaeger, J., 2013. Reverse-engineering post-transcriptional regulation of gap genes in *Drosophila melanogaster*. PLoS Comput. Biol. 9 (10), e1003281. http://dx.doi.org/10.1371/journal.pcbi.1003281.

Becker, K., Bluhm, A., Casas-Vila, N., Dinges, N., Dejung, M., Sayols, S., Kreutz, C., Roignant, J.Y., Butter, F., Legewie, S., 2018. Quantifying post-transcriptional regulation in the development of *Drosophila melanogaster*. Nat. Commun. 9 (1), 4970. http://dx.doi.org/10.1038/s41467-018-07455-9.

Bothma, J.P., Garcia, H.G., Esposito, E., Schlissel, G., Gregor, T., Levine, M., 2014. Dynamic regulation of *eve* stripe 2 expression reveals transcriptional bursts in living *Drosophila* embryos. Proc. Natl. Acad. Sci. USA 111, 10598–10603. http://dx.doi.org/10.1073/pnas.1410022111.

Bullock, S.L., Stauber, M., Prell, A., Hughes, J.R., Ish-Horowicz, D., Schmidt-Ott, U., 2004. Differential cytoplasmic mRNA localisation adjusts pair-rule transcription factor activity to cytoarchitecture in dipteran evolution. Development 131 (17), 4251–4261.

Chagnovich, D., Lehmann, R., 2001. Poly(A)-independent regulation of maternal *hunchback* translation in the *Drosophila* embryo. PNAS 98 (20), 11359–11364.

Cheng, Z., Teo, G., Krueger, S., Rock, T.M., Koh, H.W., Choi, H., Vogel, C., 2016. Differential dynamics of the mammalian mRNA and protein expression response to misfolding stress. Mol. Syst. Biol. 12, 855. http://dx.doi.org/10.15252/msb.20156423.

Cho, P.F., Gamberi, C., Cho-Park, Y.A., Cho-Park, I.B., Lasko, P., Sonenberg, N., 2006. Cap-dependent translational inhibition establishes two opposing morphogen gradients in *Drosophila* embryos. Curr. Biol. 16, 2035–2041.

Choi, H.M.T., Beck, V., Pierce, N.A., 2014. Next-generation in situ hybridization chain reaction: higher gain, lower cost, greater durability. ACS Nano 8, 4284–4294. http://dx.doi.org/10.1021/nn405717p.

Clark, E., 2017. Dynamic patterning by the *Drosophila* pair-rule network reconciles long-germ and short-germ segmentation. PLoS Biol. 15 (9), e2002439. http://dx.doi.org/10.1371/journal.pbio.2002439.

Clyde, D.E., Corado, M.S., Wu, X., Pare, A., Papatsenko, D., Small, S., 2003. A self-organizing system of repressor gradients establishes segmental complexity in *Drosophila*. Nature 426, 849–853.

Damen, W.G.M., 2007. Evolutionary conservation and divergence of the segmentation process in arthropods. Dev. Dyn. 236, 1379–1391.

Driever, W., Nusslein-Volhard, C., 1989. The *bicoid* protein is a positive regulator of *hunchback* transcription in the early *Drosophila* embryo. Nature 337, 138–143.

Dubnau, J., Struhl, G., 1996. RNA recognition and translational regulation by a homeodomain protein. Nature 379 (6567), 694–699.

El-Sherif, E., Levine, M., 2016. Shadow enhancers mediate dynamic shifts of gap gene expression in the *Drosophila* embryo. Curr. Biol. 26, 1164–1169.

Fowlkes, C.C., Eckenrode, K.B., Bragdon, M.D., Meyer, M., Wunderlich, Z., Simirenko, L., Luengo Hendriks, C.L., Keränen, S.V., Henriquez, C., Knowles, D.W., Biggin, M.D., Eisen, M.B., DePace, A.H., 2011. A conserved developmental patterning network produces quantitatively different output in multiple species of *Drosophila*. PLoS Genet. 7 (10), e1002346. http://dx.doi.org/10.1371/journal.pgen.1002346.

Fujioka, M., Yusibova, G.L., Patel, N.H., Brown, S.J., Jaynes, J.B., 2002. The repressor activity of even-skipped is highly conserved, and is sufficient to activate *engrailed* and to regulate both the spacing and stability of parasegment boundaries. Development 129 (19), 4411–4421.

Fukaya, T., Lim, B., Levine, M., 2016. Enhancer control of transcriptional bursting. Cell 166, 1–11. http://dx.doi.org/10.1016/j.cell.2016.05.025.

Gaul, U., Seifert, E., Schuh, R., Jackle, H., 1987. Analysis of Kruppel protein distribution during early *Drosophila* development reveals posttranscriptional regulation. Cell 50, 639–647.

Goto, T., Macdonald, P., Maniatis, T., 1989. Early and late periodic patterns of *even skipped* expression are controlled by distinct regulatory elements that respond to different spatial cues. Cell 57 (3), 413–422.

Harding, K., Hoey, T., Warrior, R., Levine, M., 1989. Autoregulatory and gap gene response elements of the *even-skipped* promoter of *Drosophila*. EMBO J. 8 (4), 1205–1212.

Jaeger, J., 2011. The gap gene network. Cell. Mol. Life Sci. 68 (2), 243–274. http://dx.doi.org/10.1007/s00018-010-0536-y.

Jaeger, J., Manu, Reinitz J., 2012. *Drosophila* blastoderm patterning. Curr. Opin. Genet. Dev. 22 (6), 533–541. http://dx.doi.org/10.1016/j.gde.2012.10.005.

Jaeger, J., Surkova, S., Blagov, M., Janssens, H., Kosman, D., Kozlov, K.N., Manu, Myasnikova, E., Vanario- Alonso, C.E., Samsonova, M., Sharp, D.H., Reinitz, J., 2004. Dynamic control of positional information in the early *Drosophila* embryo. Nature 430 (6997), 368–371.

Janssens, H., Hou, S., Jaeger, J., Kim, A.R., Myasnikova, E., Sharp, D., Reinitz, J., 2006. Quantitative and predictive model of transcriptional control of the *Drosophila melanogaster even skipped gene*. Nat. Genet. 38, 1159–1165.

Jovanovic, M., Rooney, M.S., Mertins, P., Przybylski, D., Chevrier, N., Satija, R., Rodriguez, E.H., Fields, A.P., Schwartz, S., Raychowdhury, R., Mumbach, M.R., Eisenhaure, T., Rabani, M., Gennert, D., Lu, D., Delorey, T., Weissman, J.S., Carr, S.A., Hacohen, N., Regev, A., 2015. Immunogenetics. Dynamic profiling of the protein life cycle in response to pathogens. Science 347 (6226), 1259038. http://dx.doi.org/10.1126/science.1259038.

Koussounadis, A., Langdon, S.P., Um, I.H., Harrison, D.J., Smith, V.A., 2015. Relationship between differentially expressed mRNA and mRNA-protein correlations in a xenograft model system. Sci. Rep. 5, 10775. http://dx.doi.org/10.1038/srep10775.

Kozlov K., 2008. ProStack: a new platform for image analysis, CSHL Conference. Computational Cell Biology, March 24–31, 2008.
Kozlov, K., Surkova, S., Myasnikova, E., Reinitz, J., Samsonova, M., 2012. Modeling of gap gene expression in *Drosophila Kruppel* mutants. PLoS Comput. Biol. 8, e1002635. http://dx.doi.org/10.1371/journal.pcbi.1002635.
Lasko, P., 2011. Posttranscriptional regulation in *Drosophila* oocytes and early embryos. Wiley Interdiscip. Rev. RNA 2 (3), 408–416. http://dx.doi.org/10.1002/wrna.70.
Li, J.J., Bickel, P.J., Biggin, M.D., 2014. System wide analyses have underestimated protein abundances and the importance of transcription in mammals. PeerJ 2, e270. http://dx.doi.org/10.7717/peerj.270.
Liu, Y., Beyer, A., Aebersold, R., 2016. On the dependency of cellular protein levels on mRNA abundance. Cell 165 (3), 535–550. http://dx.doi.org/10.1016/j.cell.2016.03.014.
Maier, T., Guell, M., Serrano, L., 2009. Correlation of mRNA and protein in complex biological samples. FEBS Lett. 583, 3966–3973. http://dx.doi.org/10.1016/j.febslet.2009.10.036.
Maier, T., Schmidt, A., Güell, M., Kühner, S., Gavin, A.C., Aebersold, R., Serrano, L., 2011. Quantification of mRNA and protein and integration with protein turnover in a bacterium. Mol. Syst. Biol. 7, 511. http://dx.doi.org/10.1038/msb.2011.38.
Nagaso, H., Murata, T., Day, N., Yokoyama, K.K., 2001. Simultaneous detection of RNA and protein by in situ hybridization and immunological staining. J. Histochem. Cytochem. 49, 1177–1182.
Niessing, D., Blanke, S., Jaeckle, H., 2002. Bicoid associates with the 5-cap-bound complex of *caudal* mRNA and represses translation. Genes Dev. 16, 2576–2582.
Peshkin, L., Wühr, M., Pearl, E., Haas, W., Freeman, R.M., Jr., Gerhart, J.C., Klein, A.M., Horb, M., Gygi, S.P., Kirschner, M.W., 2015. On the relationship of protein and mRNA dynamics in vertebrate embryonic development. Dev. Cell. 35 (3), 383–394. http://dx.doi.org/10.1016/j.devcel.2015.10.010, (2015 Nov 9).
Rivera-Pomar, R., Niessing, D., Schmidt-Ott, U., Gehring, W.J., Jäckle, H., 1996. RNA binding and translational suppression by *bicoid*. Nature 379 (6567), 746–749.
Schwanhäusser, B., Busse, D., Li, N., Dittmar, G., Schuchhardt, J., Wolf, J., Chen, W., Selbach, M., 2011. Global quantification of mammalian gene expression control. Nature 473 (7347), 337–342. http://dx.doi.org/10.1038/nature10098.
Small, S., Blair, A., Levine, M., 1996. Regulation of two pair-rule stripes by a single enhancer in the *Drosophila* embryo. Dev. Biol. 175, 314–324.
Sonoda, J., Wharton, R., 1999. Recruitment of Nanos to *hunchback* mRNA by Pumilio. Genes Dev. 13, 2704–2712.
de Sousa Abreu, R., Penalva, L.O., Marcotte, E.M., Vogel, C., 2009. Global signatures of protein and mRNA expression levels. Mol. Biosyst. 5 (12), 1512–1526. http://dx.doi.org/10.1039/b908315d.
Staller, M.V., Vincent, B.J., Bragdon, M.D., Lydiard-Martin, T., Wunderlich, Z., Estrada, J., DePace, A.H., 2015. Shadow enhancers enable Hunchback bifunctionality in the *Drosophila* embryo. Proc. Natl. Acad. Sci. USA 112 (3), 785–790. http://dx.doi.org/10.1073/pnas.1413877112.
Struffi, P., Corado, M., Kaplan, L., Yu, D., Rushlow, C., Small, S., 2011. Combinatorial activation and concentration-dependent repression of the *Drosophila even skipped* stripe 3+7 enhancer. Development 138 (19), 4291–4299. http://dx.doi.org/10.1242/dev.065987.
Surkova, S., Kosman, D., Kozlov, K., Myasnikova, E., Samsonova, A.A., Spirov, A., Vanario-Alonso, C.E., Samsonova, M., Reinitz, J., 2008a. Characterization of the *Drosophila* segment determination morphome. Dev. Biol. 313 (2), 844–862.
Surkova, S., Myasnikova, E., Janssens, H., Kozlov, K.N., Samsonova, A.A., Reinitz, J., Samsonova, M., 2008b. Pipeline for acquisition of quantitative data on segmentation gene expression from confocal images. FLY 2 (2), 58–66.
Surkova, S., Golubkova, E., Manu, Panok, L., Mamon, L., Reinitz, J., Samsonova, M., 2013. Quantitative dynamics and increased variability of segmentation gene expression in the *Drosophila Kruppel* and *knirps* mutants (2013). Dev. Biol. 376, 99–112. http://dx.doi.org/10.1016/j.ydbio.2013.01.008.
Tautz, D., Nigro, L., 1998. Microevolutionary divergence pattern of the segmentation gene *hunchback* in *Drosophila*. Mol. Biol. Evol. 15 (11), 1403–1411.
Vogel, C., Marcotte, E.M., 2012. Insights into the regulation of protein abundance from proteomic and transcriptomic analyses. Nat. Rev. Genet. 13 (4), 227–232. http://dx.doi.org/10.1038/nrg3185.
Wieschaus, E., Nusslein-Volhard, C., Kluding, H., 1984. *Kruppel*, a gene whose activity is required early in the zygotic genome for normal embryonic segmentation. Dev. Biol. 104, 172–186.
Wu, X., Vasisht, V., Kosman, D., Reinitz, J., Small, S., 2001. Thoracic patterning by the *Drosophila* gap gene *hunchback*. Dev. Biol. 237, 79–92.
Xu, H., Sepúlveda, L.A., Figard, L., Sokac, A.M., Golding, I., 2015. Combining protein and mRNA quantification to decipher transcriptional regulation. Nat. Methods 740 (8), 12. http://dx.doi.org/10.1038/nmeth.3446.